BJP British Journal of Pharmacology

DOI:10.1111/j.1476-5381.2012.02106.x
www.brjpharmacol.org

RESEARCH PAPER

Rosuvastatin prevents angiotensin II-induced vascular changes by inhibition of NAD(P)H oxidase and COX-1

Rocchina Colucci[1], Matteo Fornai[1], Emiliano Duranti[1], Luca Antonioli[1], Ilaria Rugani[1], Fatma Aydinoglu[1], Chiara Ippolito[2], Cristina Segnani[2], Nunzia Bernardini[2], Stefano Taddei[1], Corrado Blandizzi[1] and Agostino Virdis[1]

[1]*Department of Internal Medicine, University of Pisa, Pisa, Italy, and* [2]*Department of Human Morphology and Applied Biology, University of Pisa, Pisa, Italy*

Correspondence
Agostino Virdis, Department of Internal Medicine, University of Pisa, Via Roma 67, 56100 Pisa, Italy. E-mail: agostino.virdis@med.unipi.it

Dr. Bernardini was the coordinator of the morphological and immunohistochemical studies.

Keywords
angiotensin II; endothelium; extracellular matrix; microcirculation; oxidant stress

Received
20 February 2012
Revised
7 June 2012
Accepted
2 July 2012

BACKGROUND AND PURPOSE

NAD(P)H oxidase and COX-1 participate in vascular damage induced by angiotensin II. We investigated the effect of rosuvastatin on endothelial dysfunction, vascular remodelling, changes in extracellular matrix components and mechanical properties of small mesenteric arteries from angiotensin II-infused rats.

EXPERIMENTAL APPROACH

Male rats received angiotensin II (120 ng·kg^{-1}·min^{-1}, subcutaneously) for 14 days with or without rosuvastatin (10 mg·kg^{-1}·day^{-1}, oral gavage) or vehicle. Vascular functions and morphological parameters were assessed by pressurized myography.

KEY RESULTS

In angiotensin II-infused rats, ACh-induced relaxation was attenuated compared with controls, less sensitive to L-NAME, enhanced by SC-560 (COX-1 inhibitor) or SQ-29548 (prostanoid TP receptor antagonist), and normalized by the antioxidant ascorbic acid or NAD(P)H oxidase inhibitors. After rosuvastatin, relaxations to ACh were normalized, fully sensitive to L-NAME, and no longer affected by SC-560, SQ-29548 or NAD(P)H oxidase inhibitors. Angiotensin II enhanced intravascular superoxide generation, eutrophic remodelling, collagen and fibronectin depositions, and decreased elastin content, resulting in increased vessel stiffness. All these changes were prevented by rosuvastatin. Angiotensin II increased phosphorylation of NAD(P)H oxidase subunit p47phox and its binding to subunit p67phox, effects inhibited by rosuvastatin. Rosuvastatin down-regulated vascular Nox4/NAD(P)H isoform and COX-1 expression, attenuated the vascular release of 6-keto-PGF$_{1\alpha}$, and enhanced copper/zinc-superoxide dismutase expression.

CONCLUSION AND IMPLICATIONS

Rosuvastatin prevents angiotensin II-induced alterations in resistance arteries in terms of function, structure, mechanics and composition. These effects depend on restoration of NO availability, prevention of NAD(P)H oxidase-derived oxidant excess, reversal of COX-1 induction and its prostanoid production, and stimulation of endogenous vascular antioxidant defences.

Abbreviations

Ang, angiotensin; Cu/Zn-SOD, copper/zinc-superoxide dismutase; DHE, dihydroethidium; ECM, extracellular matrix; ROS, reactive oxygen species; SNP, sodium nitroprusside

Introduction

Angiotensin (Ang) II plays a critical role in the development of endothelial dysfunction and structural alterations (vascular remodelling) in small resistance arteries, mainly through increased generation of reactive oxygen species (ROS), driven by NAD(P)H oxidase activation (Touyz, 2005). NAD(P)H oxidase comprises the membrane-bound catalytic subunits Nox and p22phox, associated with several cytosolic regulatory subunits (Paravicini and Touyz, 2008). Recently, multiple homologues of Nox were found and Nox1, Nox2 and Nox4 were identified in vascular tissues (Ago *et al.*, 2004). In turn, the Ang II-induced ROS generation leads to a reduction of NO availability, increase in cell growth and changes in extracellular matrix (ECM) proteins. In particular, increased collagen and fibronectin deposition, together with decreased elastin content, have been found in the media of mesenteric resistance arteries from Ang II-infused animals (Neves *et al.*, 2003; 2004; Brassard *et al.*, 2005; Virdis *et al.*, 2012). COX-1 actively participates in Ang II-induced vascular alterations. In small arteries from Ang II-treated animals, COX-1 is over-expressed and its derived prostanoid(s) contribute to the Ang II-mediated endothelial dysfunction (Virdis *et al.*, 2007), remodelling, changes in mechanical properties and ECM composition of the extracellular matrix (ECM) (Virdis *et al.*, 2012).

Inhibitors of 3-hydroxy-3-methylglutaryl-CoA reductase (statins) can exert lipid-independent, vascular protective effects at several stages of the atherosclerotic process, including endothelial dysfunction (de Sotomayor *et al.*, 2005; Virdis *et al.*, 2009) and plaque area (Calkin *et al.*, 2008). Most of these effects depend on their antioxidant actions. Specifically, rosuvastatin was previously shown to prevent NAD(P)H oxidase-derived ROS generation (Sicard *et al.*, 2007; Whaley-Connell *et al.*, 2008; Kang and Mehta, 2009), leading to a renoprotective effect or to an attenuated aortic plaque deposition (Calkin *et al.*, 2008; Whaley-Connell *et al.*, 2008).

At present, it remains undetermined whether rosuvastatin may protect resistance arteries against hypertension-induced vascular changes, and the possible involvement of NAD(P)H oxidase and COX-1 pathways in such beneficial effects. For this purpose, we employed the Ang II-infused rat model, which is characterized by arterial remodelling and fibrosis resulting from NAD(P)H oxidase-induced ROS generation and vascular COX-1 over-expression (Touyz and Schiffrin, 2000; Virdis *et al.*, 2012), in the absence of lipid disorders, to assess the net effects of rosuvastatin on endothelial dysfunction, vascular remodelling, mechanical changes and alterations in ECM components of resistance mesenteric arteries. The inhibition of NAD(P)H oxidase Nox subunits and COX-1, as possible mechanisms targeted by rosuvastatin, was also assessed.

Methods

Animals

All animal care and experimental procedures were in accordance with the European Union Council Directive 86–609, recognized by the Italian Government. The results of all studies involving animals are reported in accordance with the ARRIVE guidelines for reporting experiments involving animals (McGrath *et al.*, 2010). The total number of animals used in these experiments was 104. Under anaesthesia with chloral hydrate, male Sprague-Dawley rats (250–300 g) were implanted subcutaneously with osmotic minipumps (Alzet Corp., Palo Alto, CA, USA) to infuse Ang II (120 ng·kg^{-1}·min^{-1}; Peninsula, Palo Alto, CA, USA) or saline. Animals were treated with rosuvastatin (10 mg·kg^{-1}·day^{-1} by oral gavage; Astra Zeneca, Milan, Italy) or vehicle (n = 8 per group) for 2 weeks. The dose of rosuvastatin was selected according to preliminary dose-titration functional experiments (5–10–20 mg·kg^{-1}·day^{-1}), which included also simvastatin (10–20–40 mg·kg^{-1}·day^{-1}) and atorvastatin (10–20–40 mg·kg^{-1}·day^{-1}). Beneficial effects on endothelial function and vascular remodelling were obtained with each statin at different dosages. Rosuvastatin was able to elicit maximal functional effects at a lower dose (10 mg·kg^{-1}), compared with the others, according to its higher potency (Supporting Information Table S1). BP was measured by the tail-cuff method, as previously described (Virdis *et al.*, 2005).

Preparation and mounting of small mesenteric arteries

Immediately after death (overdose of chloral hydrate 50 mg kg^{-1} i.p.), a third-order branch of the mesenteric arterial tree was dissected and mounted on a pressurized myograph, as previously described (Virdis *et al.*, 2005). Endothelium-dependent and -independent relaxations were assessed by measuring the dilator responses of mesenteric arteries to cumulative concentrations of ACh (0.001–100 μM; Sigma Chemicals, St Louis, MO, USA) and sodium nitroprusside (SNP, 0.01–100 μM; Sigma,), respectively, in vessels precontracted with norepinephrine (10 μM).

To assess mechanical properties, intraluminal pressure was increased step-wise from 3 to 140 mmHg. Media thickness and lumen diameter were measured at each pressure level (see Supporting Information Appendix S1).

Influence of COX-1, COX-2 and prostanoid TP receptors on endothelium-dependent relaxation

The participation of COX-1 and COX-2 isoenzymes on endothelial function was investigated by assessing ACh-induced relaxations after 30 min pre-incubation with the COX-1 inhibitor SC-560 (1 μM, Sigma) or the COX-2 inhibitor Dup-697 (1 μM; Tocris Bioscience, Minneapolis, MN, USA). The contribution of TP receptors was assessed by repeating ACh after 30 min incubation with the TP receptor antagonist SQ-29548 (1 μM; Cayman Chemical, Ann Arbor, MI, USA; receptor nomenclature follows Alexander *et al.*, 2011). Then, to test the possibility that isoprostanes formed non-enzymatically could activate TP receptors independently from COX-derived prostanoids, ACh was applied during simultaneous incubation with SC-560 and SQ-29548.

Influence of NO availability, ROS generation and NAD(P)H oxidase inhibition on endothelium-dependent relaxation

The role of NO and the influence of ROS were investigated by repeating the ACh stimulation after 30 min pre-incubation with the NO synthase inhibitor L-NAME (100 μM; Sigma),

ascorbic acid (100 μM; Sigma) or their simultaneous incubation. In additional vessels from Ang II-treated rats ($n = 6$), the role of NAD(P)H oxidase on NO availability was investigated by assessing the effects of ACh infusion after 30 min incubation with two different NAD(P)H oxidase inhibitors, apocynin (10 μM; Sigma) and diphenylene iodinium (DPI, 10 μM; Sigma) (Paravicini and Touyz, 2008), as well as during their incubation with L-NAME. Finally, to investigate whether rosuvastatin can exert beneficial acute functional effects, concentration–response curves to ACh and SNP were constructed in vessels from Ang II-treated rats ($n = 6$), following 1 h incubation with increasing concentrations of rosuvastatin (0.01–1 μM).

In situ *detection of superoxide anion*

The *in situ* production of superoxide anion from frozen mesenteric vessel sections (30 μm) was evaluated by means of the fluorescent dye dihydroethidium (DHE, Sigma), as previously described (Virdis *et al.*, 2003). Three slides per segment were analysed simultaneously after incubation with Krebs solution (see Supporting Information Appendix S1) at 37°C for 30 min. Krebs-HEPES buffer containing 2 μM DHE was then applied to each section and evaluated under fluorescence microscopy. The percentage of arterial wall area stained with the red signal was estimated using an imaging software (McBiophotonics Image J; National Institutes of Health, Bethesda, MD, USA).

Immunostaining of type I collagen and fibronectin, and histochemical detection of elastin

After dissection, small mesenteric arteries were immediately fixed in cold 4% paraformaldehyde and paraffin-embedded at 56°C. About 8-μm-thick sections were immunostained by rabbit polyclonal anti-type I collagen (1:1500; Abcam, Cambridge, UK) and rabbit monoclonal anti-fibronectin (1:10000; Epitomics, Burlingame, CA, USA) antibodies, as previously reported (Virdis *et al.*, 2012). Histochemistry for elastic fibres was performed by the Tänzer–Unna orcein staining (1% orcein in acid alcohol) (Bostom *et al.*, 1999). To assess the effects of COX-1 and NAD(P)H oxidase inhibition on Ang II-induced vascular collagen deposition, two additional groups of Ang II-infused rats received SC-560 (5 $mg \cdot kg^{-1} \cdot day^{-1}$, oral gavage) or apocynin (1.5 $mmol \cdot L^{-1}$, in drinking water) for two weeks ($n = 8$ each group). The doses of SC-560 and apocynin were selected on the basis of previous reports (Beswick *et al.*, 2001; Virdis *et al.*, 2012) and according to the amount of water consumed by the rats. In the whole artery section, the percentage of labelled wall area was quantified by means of an image analysis software (McBiophotonics Image J) and normalized to the total area examined.

Immunoprecipitation of NAD(P)H oxidase subunit p47phox and immunoblotting of phosphoserine, p67phox and p47phox

Immunoprecipitation and immunoblotting were used to assess phosphorylation of the NAD(P)H oxidase subunit p47phox and its binding to the subunit p67phox, as indexes of NAD(P)H oxidase activation (Li and Shah, 2003). Briefly, arterial specimens were homogenized in RIPA lysis buffer. The homogenates were centrifuged (20,000 x *g* for 15 min at 4°C). and supernatants were separated from pellets and stored at –80°C. Protein concentration was determined by Bradford method (Protein Assay Kit; Bio-Rad, Hercules, CA, USA). To perform co-immunoprecipitation analysis, equivalent amounts of proteins (250 μg) were immunoprecipitated with anti-p47phox antibody conjugated with protein A/G agarose beads (Li *et al.*, 2002; Li and Shah, 2003). The obtained immunoblots were incubated with mouse monoclonal anti-phosphoserine antibody, rabbit anti-p67phox antibody and rabbit polyclonal anti-p47phox antibody (Sigma). ImmunoCruz Optima IP/Western Blot reagent kit (Santa Cruz, CA, USA) was used to improve the detection of immunoprecipitated proteins. Immunoreactive bands were visualized by chemiluminescent reagents, exposed to Kodak Image Station 440 for signal detection and scanned densitometrically for quantification of signal.

Real-time PCR

Real-time PCR (RT-PCR) assays were employed to detect Nox1, Nox2, Nox4 and COX-1 mRNA expression in mesenteric arteries (see Supporting Information Appendix S1).

Western blot analysis

Western blot analysis was carried out to detect copper/zinc-superoxide dismutase (Cu/Zn-SOD) and COX-1 protein expression in rat mesenteric arteries (see Supporting Information Appendix S1).

6-Keto-PGF$_{1\alpha}$ and 8-isoprostane assay

6-Keto-PGF$_{1\alpha}$ was assayed as stable metabolite of COX-1-derived prostacyclin, and 8-isoprostane as COX-2-derived prostanoid (Virdis *et al.*, 2009; 2012). Concentrations of 6-keto-PGF$_{1\alpha}$ and 8-isoprostane were determined in the incubation medium of isolated mesenteric vessels from all groups by means of enzyme immunoassay commercial kits (Cayman).

Determination of serum cholesterol and plasma malondialdehyde, aldosterone and catecholamine assays

Venous blood samples were taken immediately after death. For cholesterol, blood was allowed to clot and serum was separated by centrifugation and stored at –70°C. Total serum cholesterol was assayed by a enzymic method (Roche, Penzberg, Germany). For plasma malondialdehyde and aldosterone, the anticoagulant was 6% EDTA; for plasma catecholamine we used 10% EGTA. The colorimetric assessment of malondialdehyde levels was performed by commercial kit. Plasma aldosterone was assayed by radioimmunoassay (DiaSorin, Saluggia, Italy). Plasma epinephrine and norepinephrine levels were determined by HPLC (Bernini *et al.*, 2008).

Data analysis

Results are presented as mean ± SEM and analysed by ANOVA, followed by Student-Newman–Keuls test, or by Student's *t*-test. $P < 0.05$ was considered significant. Maximal ACh- and SNP-induced relaxant responses (E_{max}) were calculated as maximal percentage increments of lumen diameter. *n* indicates the number of animals in each assay.

Results

BP, plasma analytes and morphology of mesenteric resistance arteries

BP was monitored throughout the treatment period (see Supporting Information Figure S1). Both systolic and diastolic BPs were increased by Ang II. Rosuvastatin slightly affected systolic BP, while significantly reducing diastolic BP, and consequently, mean BP (Table 1). Plasma cholesterol was significantly reduced by rosuvastatin in both groups. Plasma aldosterone was significantly increased in Ang II-infused rats and unaffected by rosuvastatin (Table 1). Plasma epinephrine and norepinephrine levels were similar in all groups (Table 1). Ang II decreased the lumen diameter and increased the media thickness of mesenteric resistance arteries, resulting in an increased media/lumen ratio (Table 1). Ang II enhanced also the growth index, indicating some degree of hypertrophic remodelling, even though the slight increase in media cross-sectional area did not achieve statistical significance. All the Ang II-induced changes were reversed by rosuvastatin (Table 1).

Effects of COX-1, COX-2 and TP receptor antagonism on endothelial function

In control rats, relaxation to ACh was not affected by SC-560, Dup-697 or SQ-29548 (Figure 1A). By contrast, vessels from Ang II animals showed an attenuated relaxation to ACh ($P < 0.001$ vs. controls), which was unaffected by Dup-697, but significantly improved, although not normalized, by SC-560 or SQ-29548 ($P < 0.05$ vs. controls, Figure 1B). When SC-560 and SQ-29548 were simultaneously applied, no further increase in response to ACh was obtained (ACh, E_{max}: 63.0 ± 1.2%; ACh plus SC-560 and SQ-29548, 85.6 ± 1.1%; $P < 0.001$ vs. ACh alone; not significant vs. ACh plus SC-560 or SQ-29548).

Effects of NOS antagonism, ROS scavenging and NAD(P)H oxidase inhibition on endothelial function

In control animals, the relaxation to ACh was significantly blunted by L-NAME and not affected by ascorbic acid (Figures 1C, 2B). In Ang II-treated rats, L-NAME only slightly blunted the relaxation to ACh (Figures 1D, 2B). Ascorbic acid normalized the relaxation to ACh and restored the inhibitory effect of L-NAME (Figure 1D). As observed with ascorbic acid, apocynin normalized the relaxation to ACh (ACh, E_{max}: 63.2 ± 0.8%; ACh plus apocynin, 96.6 ± 1.1%; $P < 0.001$) and restored the inhibition by L-NAME on ACh (ACh plus apocynin and L-NAME, 65.8 ± 0.8%; inhibition: 30.8 ± 0.9%). Similar results were obtained with DPI (ACh: 63.8 ± 0.9%; ACh plus DPI, 95.9 ± 1.4%; $P < 0.001$; ACh plus DPI and L-NAME, 66.9 ± 1.2%; inhibition: 29.0 ± 1.3%).

Effect of rosuvastatin on endothelial function

Following treatment with rosuvastatin, the relaxation to ACh was normalized and no longer modified by SC-560, SQ-29548, ascorbic acid, apocynin or DPI (Figure 2A). The inhibitory effect of L-NAME on ACh-induced relaxation was also fully restored (Figure 2B). Vessels from rosuvastatin-treated control rats were similar to those from untreated controls (ACh, E_{max}: 97.2 ± 0.6%; ACh plus SC-560, 96.1 ± 0.9%; ACh plus SQ-29548, 95.8 ± 1.2%; ACh plus ascorbic acid, 96.2 ± 0.5%; ACh plus L-NAME, 58.3 ± 0.9%; inhibition: −38.9 ± 0.7%). Relaxations to SNP were similar in control and Ang II-treated animals (E_{max}: 97.2 ± 0.8% and 97.8 ± 0.9%, respectively), and not modified by rosuvastatin

Table 1

Physiological and vascular morphological parameters

Parameter	Control ($n = 8$)	Rosu ($n = 8$)	Ang II ($n = 8$)	Ang II + Rosu ($n = 8$)
Body weight, g	281 ± 20	292 ± 28	274 ± 21	283 ± 37
SBP, mmHg	111 ± 4	113 ± 3	171 ± 6*	163 ± 8
MBP, mmHg	83 ± 3	82 ± 4	119 ± 4*	108 ± 3*†
MDA, μmol·L^{-1}	7.3 ± 1.6	8.4 ± 1.8	20.1 ± 2.8*	9.4 ± 2.1†
Cholesterol, mg·L^{-1}	740 ± 30	610 ± 80‡	750 ± 40	540 ± 60‡
Aldosterone, pg·mL^{-1}	189 ± 53	176 ± 64	575 ± 86*	543 ± 92
Epinephrine, pg·mL^{-1}	394 ± 72	357 ± 62	348 ± 69	385 ± 72
Norepinephrine, pg·mL^{-1}	1057 ± 127	1104 ± 159	1179 ± 148	1036 ± 163
Lumen diameter, μm	220 ± 6	224 ± 8	181 ± 7*	198 ± 6†
Media thickness, μm	10.6 ± 0.3	10.4 ± 0.7	14.2 ± 0.3*	11.8 ± 0.4†
M/L (%)	4.9 ± 0.4	4.9 ± 0.2	7.8 ± 0.2*	6.1 ± 0.2†
Media CSA, $10^3 \times \mu m^2$	7.9 ± 0.4	7.8 ± 0.5	9.1 ± 0.7	8.1 ± 0.6
Growth index (%)	–	1.4	14.4*	1.6†

*$P < 0.01$ versus control; †$P < 0.05$ versus Ang II; ‡$P < 0.05$ versus control or Ang II.
Ang, Angiotensin; CSA, cross-sectional area; M/L, media to lumen ratio; MBP, mean BP; MDA, malondialdehyde; Rosu, Rosuvastatin; SBP, systolic BP.

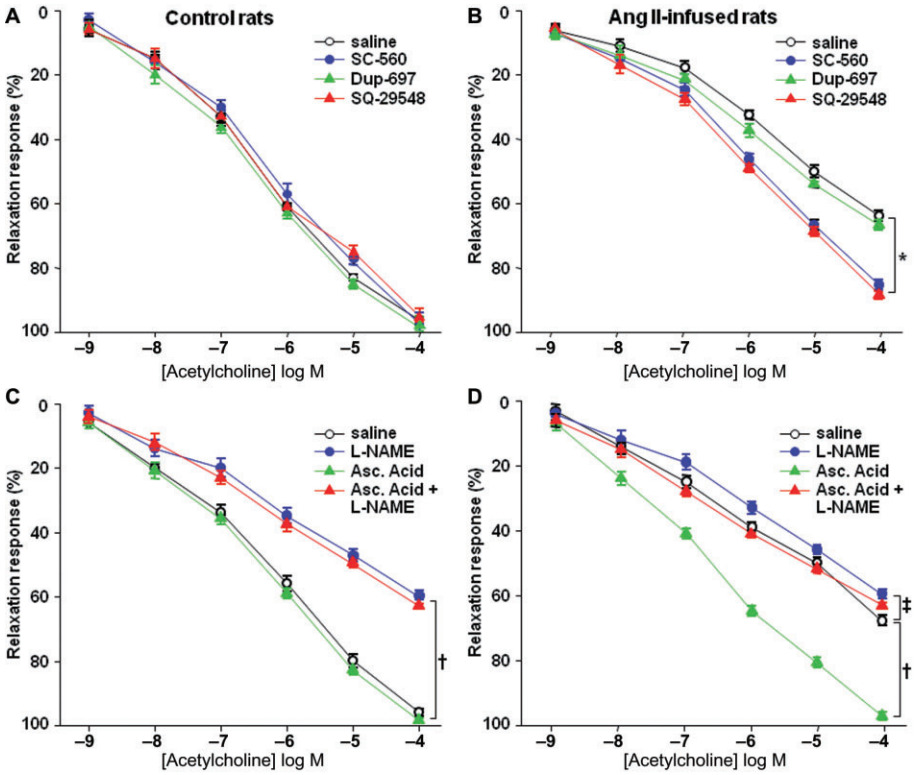

Figure 1

Relaxationsto ACh in mesenteric resistance arteries from control or Ang II rats with or without SC-560, Dup-697, SQ-29548 (A, B), or L-NAME, ascorbic acid (Asc. Acid) or both (C, D). Data are presented as means ± SEM (n = 8 per group). *P < 0.01; †P < 0.001; ‡P < 0.05.

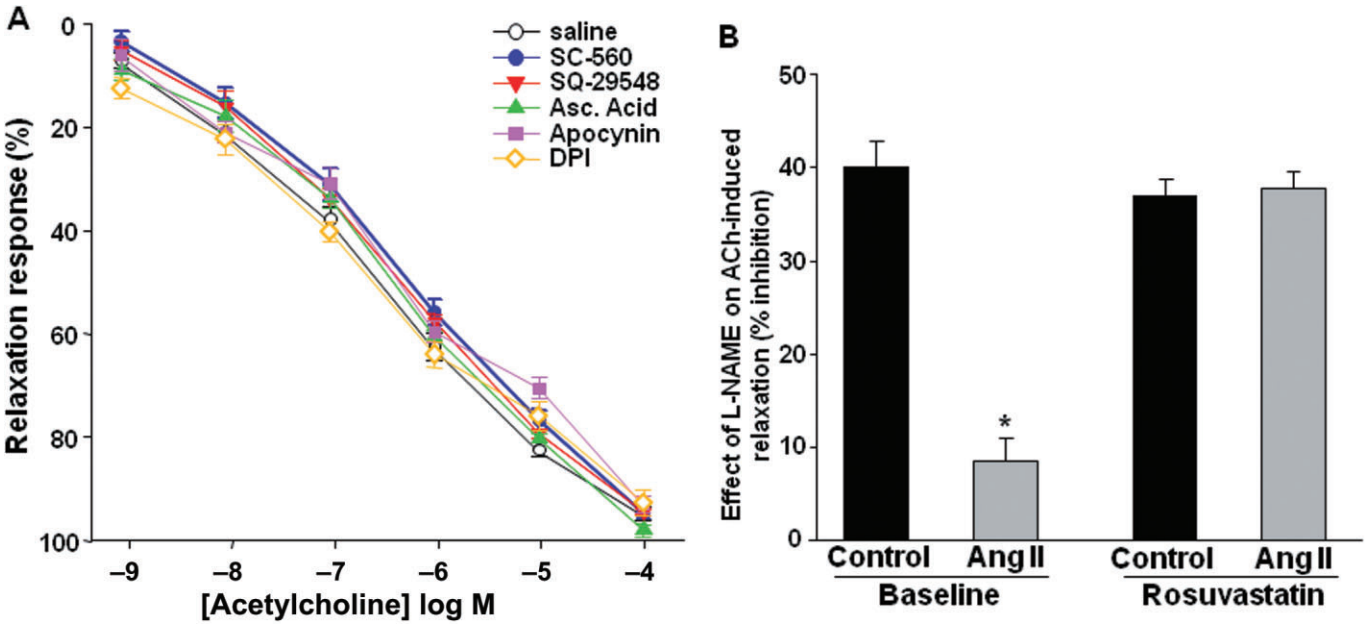

Figure 2

(A)Relaxations to ACh ± SC-560, SQ-29548, ascorbic acid, apocynin or diphenylene iodinium (DPI) in mesenteric resistance arteries from rosuvastatin-treated Ang II-infused rats. (B) Inhibition by L-NAME on maximal response to ACh in small vessels from control or Ang II rats with or without rosuvastatin. Data are presented as means ± SEM (n = 8 per group). *P < 0.001 versus other groups.

(control + rosuvastatin: 98.3 ± 1.4%; Ang II + rosuvastatin: 97.5 ± 1.1%). In arteries from Ang II-treated rats, acute rosuvastatin incubation dose-dependently ameliorated the relaxation to ACh, while the response to SNP was unaffected (Supporting Information Figure S2).

Effects of rosuvastatin on vascular superoxide generation and malondialdehyde levels

In small arteries from Ang II-treated rats, *in situ* DHE analysis revealed a dramatic increase in superoxide anion production, as compared with controls (Figure 3). The enhanced superoxide generation was abolished by rosuvastatin (Figure 3). Ang II-infused animals showed also higher plasma values of malondialdehyde, which were attenuated by rosuvastatin (Table 1).

Effect of rosuvastatin on vascular expression of type I collagen, fibronectin and elastin

Mesenteric arteries from Ang II-infused rats displayed significantly increased deposition of type I collagen and fibronectin, mainly in the outer layer of tunica media and adventitia. These effects were prevented by rosuvastatin (Figure 4; Table 2). The

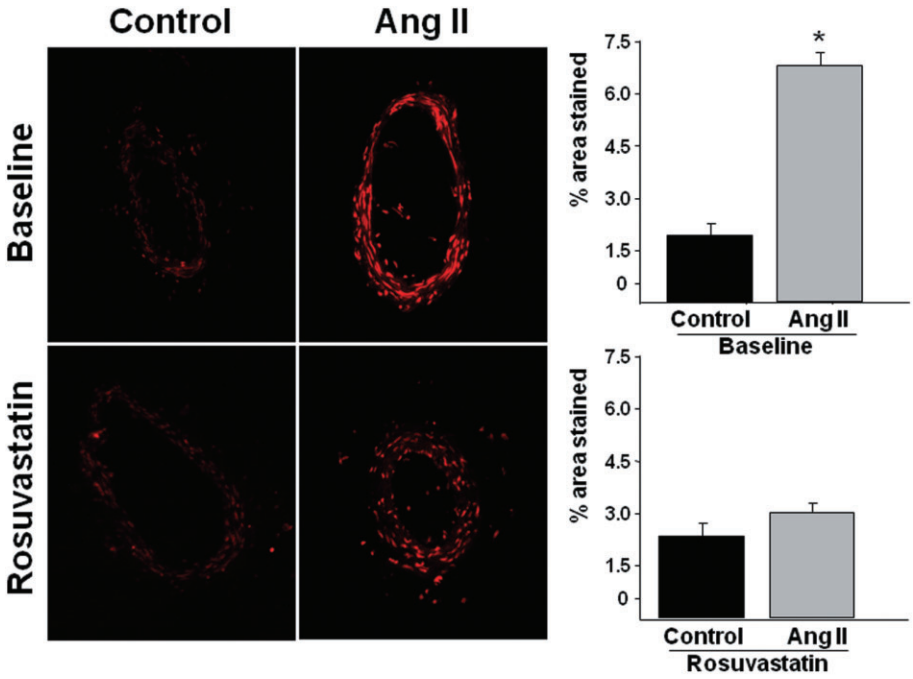

Figure 3

Representativedihydroethidium staining and quantification of the red signal (magnification ×40) in mesenteric arteries from control or Ang II-infused rats with or without rosuvastatin.. Data are presented as means ± SEM (n = 8 per group). *P < 0.01.

Table 2

Quantitative estimations of media ECM components in mesenteric arteries and 6-keto-$PGF_{1\alpha}$ and 8-isoprostane concentrations in incubation medium of isolated mesenteric vessels

Mesenteric arteries	Control (n = 8)	Rosu (n = 8)	Ang II (n = 8)	Ang II + Rosu (n = 8)	Ang II + SC-560 (n = 8)	Ang II + Apo (n = 8)
Type I collagen ($\times10^{-7}$)	20.1 ± 1.4	16.4 ± 2.2	35.8 ± 2.1*	20.3 ± 0.9	19.1 ± 1.4	20.6 ± 0.9
Fibronectin ($\times10^{-7}$)	20.5 ± 0.8	20.3 ± 1.1	26.9 ± 1.4†	21.7 ± 1.6	–	–
Elastin ($\times10^{-7}$)	32.5 ± 1.5	31.3 ± 1.9	20.6 ± 0.6*	26.4 ± 0.9	–	–
Collagen/Elastin	0.56	0.52	1.73*	0.76	–	–
6-Keto-$PGF_{1\alpha}$ ($\mu g \cdot g^{-1} \cdot mL^{-1}$)	17.1 ± 0.7	18.2 ± 0.6	41.3 ± 1.7*	22.0 ± 0.5	17.8 ± 0.9	20.4 ± 0.7
8-Isoprostane ($pg \cdot g^{-1} \cdot mL^{-1}$)	9.1 ± 1.2	8.3 ± 0.7	11.6 ± 1.1	11.1 ± 0.9	9.2 ± 1.1	12.1 ± 1.2

Values are expressed as relative intensity/area (pixels).
*P < 0.001 versus other groups; †P < 0.05 versus other groups.
Ang, Angiotensin; Apo, apocynin; Rosu, Rosuvastatin.

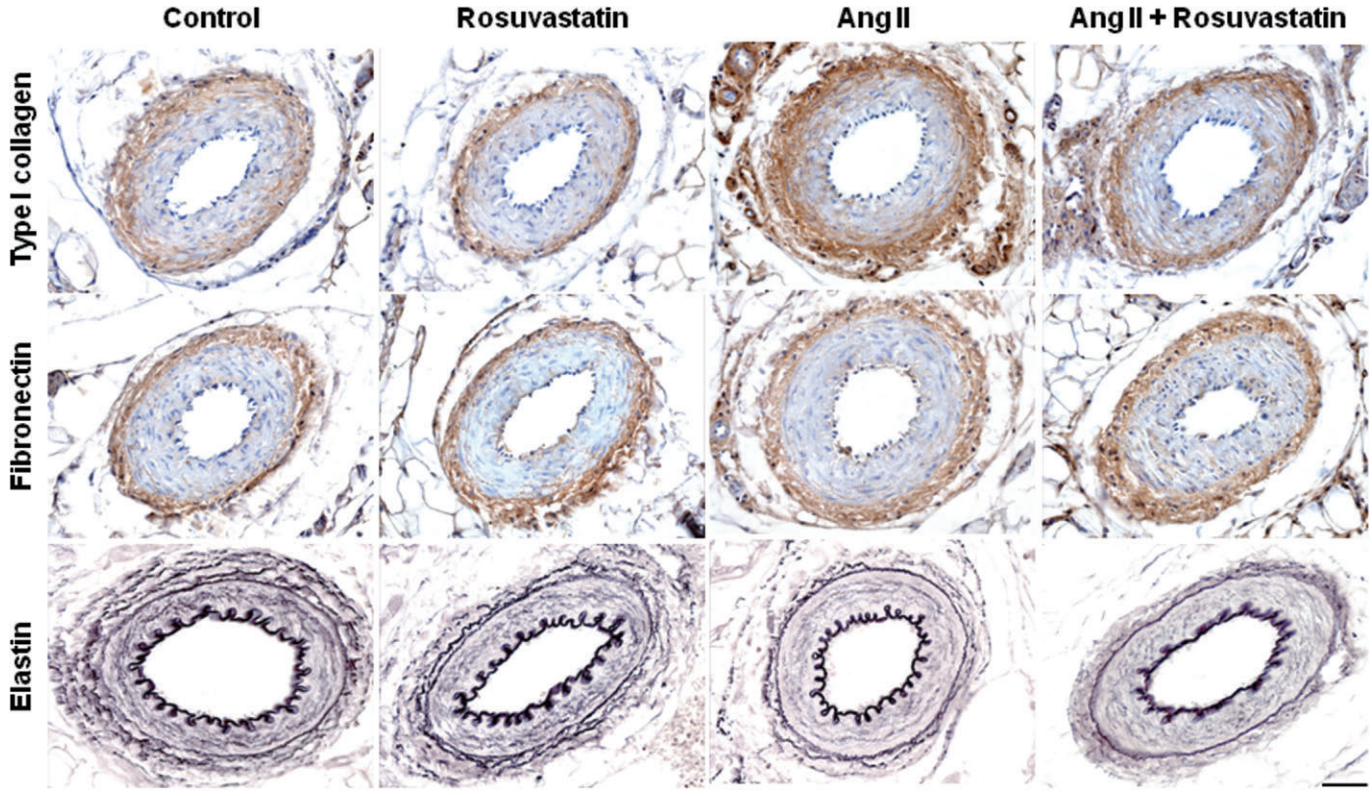

Figure 4

Representativeimages of type I collagen and fibronectin immunostaining (brown) and Tänzer–Unna orcein histochemistry for elastic fibres (black) in small mesenteric arteries from controls and Ang II-infused rats with or without rosuvastatin. Type I collagen and fibronectin in control walls were enhanced by Ang II, and prevented by rosuvastatin. Elastic fibres of internal and external elastic membranes in control arteries were reduced by Ang II and restored by rosuvastatin treatment. Scale bar: 50 μm.

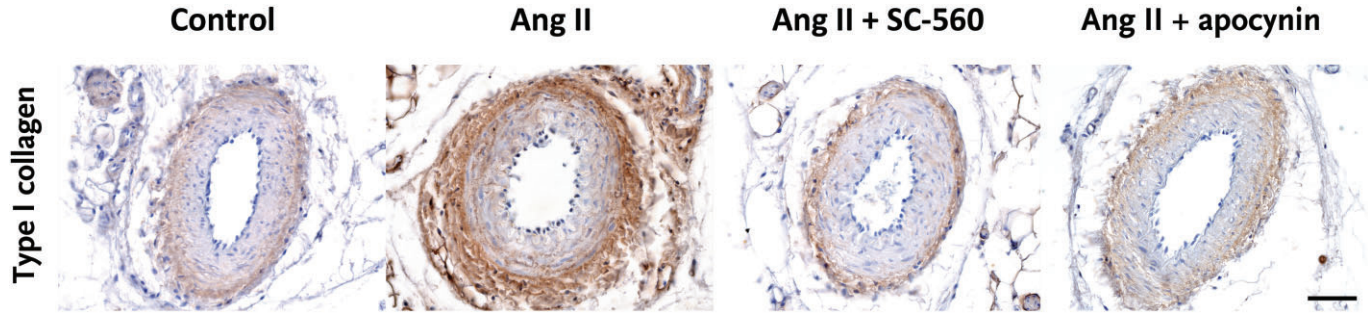

Figure 5

Representativeimages of type I collagen immunostaining (brown) in mesenteric arteries from control and Ang II-infused rats with or without SC-560 or apocynin. Ang II-induced collagen deposition was prevented by SC-560 or apocynin. Scale bar: 50 μm.

internal and external elastic membranes of control arteries displayed an elastin-rich basal wavy pattern, which was significantly reduced and deranged in Ang II-infused rats, and prevented by rosuvastatin (Figure 4; Table 2). As a consequence, the collagen-to-elastin ratio was significantly increased by Ang II and normalized after rosuvastatin (Table 2). SC-560 and apocynin were also able to prevent the Ang II-induced collagen deposition to an extent similar to that observed by rosuvastatin (Figures 4, 5; Table 2).

Vascular mechanics

In arteries from Ang II-infused rats, increments of intraluminal pressure increased the media stress to a lesser degree than in control vessels (Figure 6A). This alteration was prevented by rosuvastatin. Ang II shifted the stress–strain curve to the left, indicating the presence of increased vessel stiffness. This effect was counteracted by rosuvastatin (Figure 6B). When examined as a function of media stress, the incremental

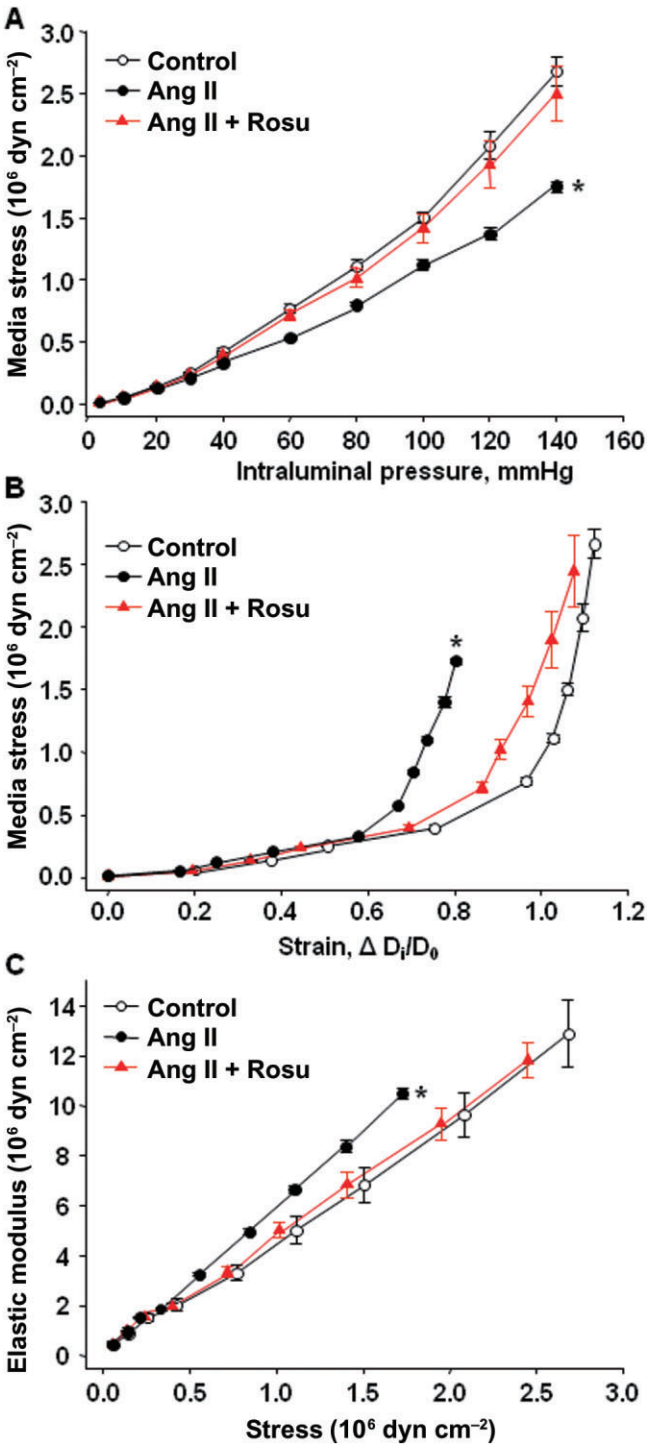

Figure 6

Mechanicalproperties of mesenteric resistance arteries. Media stress at different intraluminal pressures (A), media stress–strain relationship (B) and incremental elastic modulus plotted against media stress (C) in controls, Ang II-infused and Ang II-rosuvastatin (Rosu)-treated rats. Data are presented as means ± SEM (n = 8 per group). *P < 0.001 versus other groups (whole curve).

elastic modulus was significantly greater in Ang II group, and it was significantly ameliorated by rosuvastatin (Figure 6C).

Effects of rosuvastatin on phosphorylation of NAD(P)H oxidase subunits

The subunit p47phox was immunoprecipitated from crude homogenates of arterial specimens and serine phosphorylation of p47phox was detected by anti-phosphoserine specific antibody. Small arteries from Ang II-treated rats showed significantly increased serine phosphorylation and expression of p47phox, compared with controls and this effect was prevented by rosuvastatin. The same membranes were reprobed with anti-p67 polyclonal antibody to assess the formation of the p47phox/p67phox complex. The p67phox protein was detectable in vessels from Ang II-treated rats, but the signal disappeared after rosuvastatin treatment, indicating its ability to disrupt the Ang II-induced complex formation and counteracting the activation of NAD(P)H oxidase (Figure 7).

Effects of rosuvastatin on Nox isoforms and Cu/Zn-SOD

RT-PCR revealed that the vascular levels of Nox1, Nox2 and Nox4 mRNA expression were significantly increased by Ang II. Rosuvastatin significantly counteracted the Nox4 mRNA induction, while not affecting the Ang II-induced mRNA levels of Nox1 and Nox2 (Figure 8A). Western blot analysis showed that Ang II significantly reduced vascular Cu/Zn-SOD protein expression, and that this effect was reversed by treatment with rosuvastatin (Figure 8B).

Effect of rosuvastatin on mRNA and protein expression of COX-1

There was a low basal expression of mRNA encoding COX-1 in mesenteric arteries from control rats. Ang II infusion significantly induced mRNA COX-1 expression, which was totally prevented by rosuvastatin (Figure 9A). COX-1 protein expression was also significantly induced by Ang II, and this effect was completely prevented by rosuvastatin (Figure 9B).

6-keto-PGF$_{1\alpha}$ and 8-isoprostane production

The concentration of 6-keto-PGF$_{1\alpha}$ was higher in the incubation medium of vessels from Ang II-treated rats as compared with controls, and it was normalized by rosuvastatin (Table 2). The Ang II-induced increased production of 6-keto-PGF$_{1\alpha}$ was also significantly prevented to a similar extent by SC-560 or apocynin administrations (Table 2). A low concentration of 8-isoprostane was detected in the control group, which was not modified by Ang II, rosuvastatin, COX-1 or NAD(P)H oxidase inhibitors (Table 2).

Discussion

In the present study, mesenteric resistance arteries from Ang II-treated rats showed a reduced endothelial NO availability, secondary to a NAD(P)H oxidase-driven increased intravascular ROS generation. An increased production of COX-1-derived vasoconstrictor prostanoid, acting on TP receptors, contributed to the Ang II-induced endothelial dysfunction.

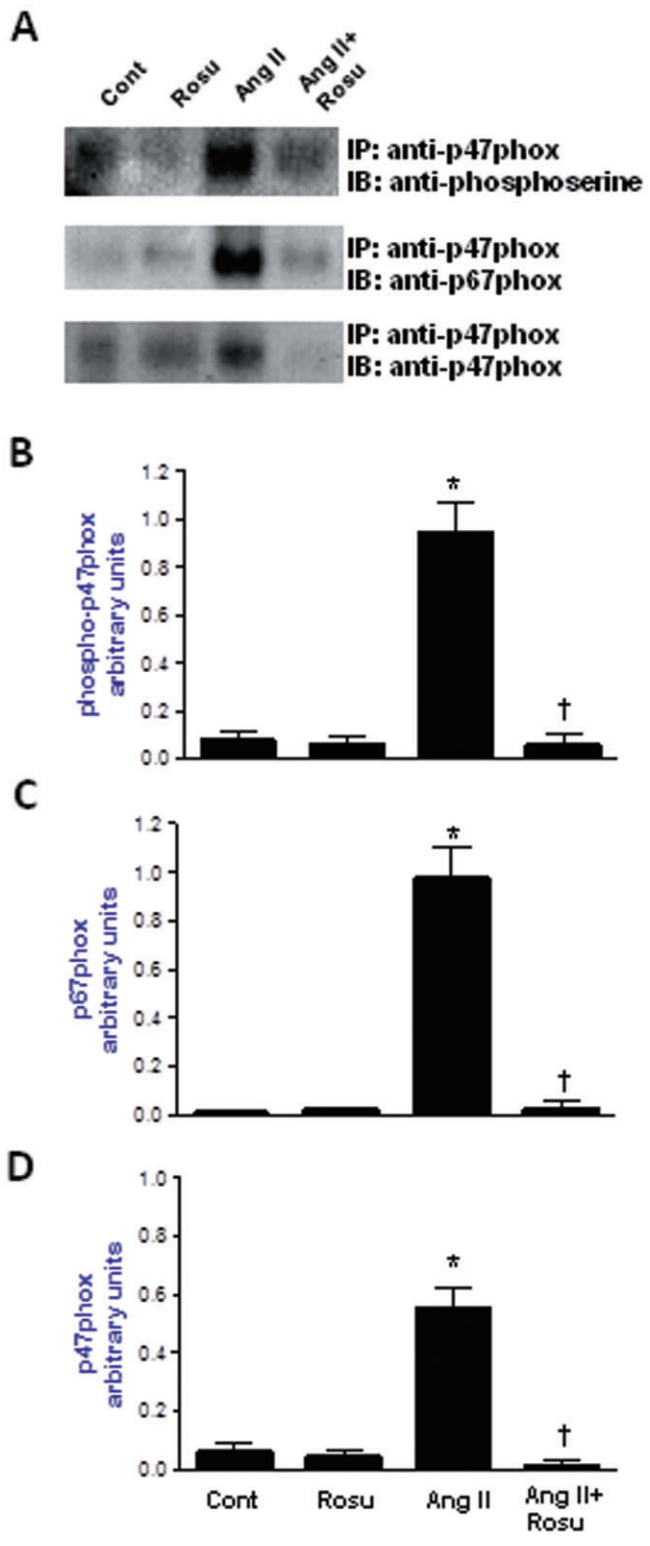

Figure 7

(A)Representative images of immunoprecipitation (IP) with anti-p47phox antibody followed by immunoblotting (IB) for phosphoserine, p67phox and p47phox in small vessels from control and Ang II-infused rats, with or without rosuvastatin (Rosu). (B) Changes in p47phox phosphorylation, p67phox binding (C) and p47phox total protein (D) were evaluated by densitometric analysis and expressed as arbitrary absorbance units. Data are presented as means ± SEM (n = 4 per group). *P < 0.05 versus control, †P < 0.05 versus Ang II.

In addition, an Ang II-mediated vascular eutrophic remodelling and an alteration in ECM composition were shown. All these findings confirm and corroborate previous results (Neves *et al.*, 2003; Brassard *et al.*, 2005; Virdis *et al.*, 2012).

Rosuvastatin normalized the endothelium-dependent relaxation, restored the inhibitory effect of L-NAME on ACh and abolished the enhancing effect of ascorbic acid or NAD(P)H inhibitors in vessels from Ang II-infused animals. Accordingly, rosuvastatin prevented also the Ang II-induced intravascular superoxide generation and normalized malondialdehyde plasma levels. These results, which represent the first major novel finding of our study, demonstrate that rosuvastatin restores the NO availability and prevents intravascular ROS generation at the level of small mesenteric arteries from Ang II-infused rats. Of note, an amelioration of endothelial dysfunction was also detected after *in vitro* incubation of vessels from Ang II-treated rats with rosuvastatin, emphasizing that the molecular mechanisms responsible for Ang II-mediated endothelial dysfunction were disrupted by this statin not only after chronic treatment, but also after acute exposure.

The second major novel finding of our study deals with the effects of rosuvastatin on vascular structural changes. Ang II elicited a predominantly eutrophic remodelling of arterial vessels, together with an increased vascular type I collagen and fibronectin depositions, and a decreased elastic fibre content, as previously documented (Virdis *et al.*, 2002; 2012; Neves *et al.*, 2003; Brassard *et al.*, 2005). All these alterations were reversed by rosuvastatin. These results provide the first demonstration that rosuvastatin can reverse the alterations of vascular structure and composition evoked by Ang II, extending to peripheral small arteries the earlier findings with rosuvastatin in renal tissue (Park *et al.*, 2009).

The stiffness of the arterial wall depends on a balance between the distensible component elastin, and the less distensible elements collagen and fibronectin (Intengan *et al.*, 1999; Intengan and Schiffrin, 2000). Accordingly, our results showed that rosuvastatin prevented the Ang II-evoked alterations in resistance artery wall mechanics. Such beneficial effects led to a significant reduction of diastolic and mean BPs. These findings, in line with a previous report (Cui *et al.*, 2009), also support the concept that the resistance vascular bed is a major determinant of diastolic BP, while only in part contributing to the systolic component. Of note, our preliminary experiments revealed that, at different dosages, simvastatin and atorvastatin were also able to ameliorate the Ang II-induced vascular changes, thus suggesting that this protective property is a class effect (see Supporting Information Table S1).

Vascular NAD(P)H oxidase activation is the main source of Ang II-mediated ROS generation (Griendling *et al.*, 1994; Fukui *et al.*, 1997; Rey *et al.*, 2001; Touyz *et al.*, 2003; Virdis *et al.*, 2004). To assess the possibility that rosuvastatin prevented vascular ROS generation by down-regulating NAD(P)H oxidase, we investigated the NAD(P)H subunit p47phox, an essential component of such enzyme in blood vessels, as previously documented (Hsich *et al.*, 2000). In our

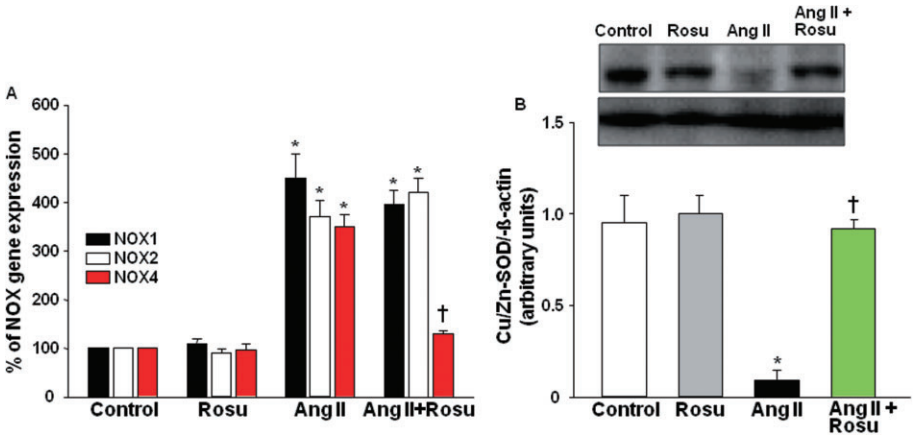

Figure 8

(A) Real-time PCR analysis of Nox1, Nox2 and Nox4 mRNA expression in mesenteric vessels from controls or Ang II-treated rats with or without rosuvastatin (Rosu). Each column represents the mean of four to six experiments ± SEM. *P < 0.05 versus control and rosuvastatin groups. †P < 0.05 versus Ang II. (B) Western blot analysis of protein products for Cu/Zn-SOD in mesenteric vessels from controls or Ang II-treated rats with or without rosuvastatin (Rosu). Panels display a representative blot and column graphs referring to the densitometric analysis of immunoreactive bands normalized to the expression of β-actin. Each column represents the mean of four to six experiments ± SEM. *P < 0.05 versus control and rosuvastatin. †P < 0.05 versus Ang II.

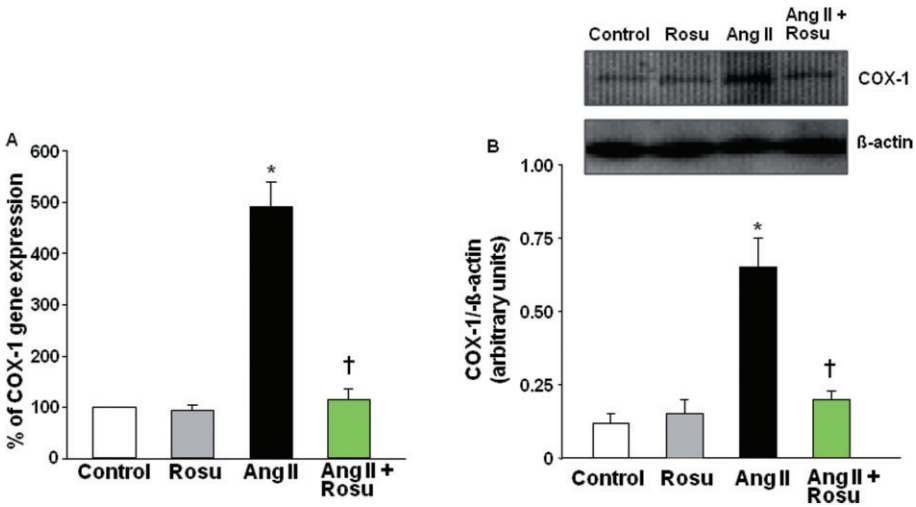

Figure 9

(A) Real-time PCR analysis of COX-1 mRNA expression in mesenteric vessels from controls or Ang II-treated rats with or without rosuvastatin (Rosu). Each column represents the mean of four to six experiments ± SEM. *P < 0.05 versus control and rosuvastatin. †P < 0.05 versus Ang II. (B) Western blot analysis of protein products for COX-1 in mesenteric vessels from controls or Ang II-treated rats with or without rosuvastatin. Panels display a representative blot and column graphs referring to the densitometric analysis of immunoreactive bands normalized to the expression of β-actin. Each column represents the mean of four to six experiments ± SEM. *P < 0.05 versus control and rosuvastatin. †P < 0.05 versus Ang II.

setting, Ang II increased the phosphorylation of p47phox, together with its binding to the subunit p67phox, and both effects were completely prevented by rosuvastatin. In particular, the vascular expression of Nox4/NAD(P)H oxidase subunit was selectively down-regulated by rosuvastatin. Concomitantly, we assessed also the endogenous vascular antioxidant defences by assaying Cu/Zn-SOD as it is the predominant isoform of SOD in rat vasculature and because it acts favourably on vascular structure (Faraci and Didion, 2004). In our model, Ang II down-regulated the expression of vascular Cu/Zn-SOD,, an effect prevented by rosuvastatin. Taken together, these findings demonstrate, for the first time, that the inhibition of ROS generation by rosuvastatin is obtained through a marked inhibition of NAD(P)H oxidase activation via a targeting of the Nox4/NAD(P)H subunit. The results from Cu/Zn-SOD assay allowed us to propose that the vascular protective effects exerted by rosuvastatin went beyond the inhibition of a major ROS source, extending to the stimulation of vascular endogenous antioxidant defences. Previous results, obtained with another statin in a similar

animal model of hypertension, corroborate our findings (Briones *et al.*, 2009; Cui *et al.*, 2009).

The inhibition of NAD(P)H oxidase is also the main mechanism whereby rosuvastatin can prevent Ang II-induced vascular fibrosis. This conclusion is supported by our results from immunohistochemistry, showing that apocynin, similar to rosuvastatin, prevented the Ang II-induced vascular collagen deposition. Accordingly, our functional data showed that rosuvastatin abolished the enhancing effects of apocynin or DPI on endothelial function.

There is evidence that COX-1 mediates Ang II-induced vascular functional and structural changes in small mesenteric vessels via production of prostacyclin acting on TP receptors (Virdis *et al.*, 2007; 2012). We evaluated the possibility that rosuvastatin might interfere with this Ang II-COX-1 interaction. After rosuvastatin treatment, endothelium-dependent relaxation was normalized and became no longer sensitive to COX-1 inhibition or antagonism at TP receptors. Rosuvastatin also dramatically down-regulated the vascular expression of COX-1 induced by Ang II and prevented the enhanced production of prostacyclin (assayed as its metabolite, 6-keto-$PGF_{1\alpha}$). The COX-1 origin of such metabolite was substantiated by our results with SC-560, which prevented its release *in vitro* from vascular tissue, As effectively as rosuvastatin. Taken together, our findings provide the first evidence that rosuvastatin down-regulates the Ang II-induced vascular over-expression of COX-1 and the related production of vasoconstrictor prostanoids. We also propose that, besides the modulation of NAD(P)H oxidase complex, the decreased COX-1 expression/activity might represent an additional target pathway whereby rosuvastatin protects the arterial wall from Ang II-induced vascular dysfunction. This is strengthened by our immunohistochemical results, showing that COX-1 inhibition by SC-560 decreased Ang II-induced vascular collagen deposition, similar to the effects of rosuvastatin. However, we cannot exclude the possibility that other COX-1 products, apart from prostacyclin, including thromboxane A_2, might be involved in the pathogenesis of Ang II-induced vascular remodelling.

An interesting issue arising from the present findings concerns a possible interaction between the two enzymic pathways, catalysed by NAD(P)H oxidase and COX-1, which are concomitantly inhibited by rosuvastatin. We observed that in Ang II-treated rats, the enhanced vascular release of 6-keto-$PGF_{1\alpha}$ was abolished by the NAD(P)H oxidase inhibitor apocynin and, similarly, by rosuvastatin, thus implying that inhibition of NAD(P)H oxidase also inhibited the COX-1-dependent prostanoid production. By contrast, levels of 8-isoprostane were not affected by any test drug. Overall, the present findings indicate that, after rosuvastatin treatment, prevention of Ang II-induced vascular dysfunction results from an attenuation of ROS generation driven by NAD(P)H oxidase activation, which in turn accounts for the restoration of NO activity and the down-regulation of COX-1 expression and function. This view is supported by a previous report on aorta from SHR, where the production of COX-1-derived endoperoxides via ROS generation was documented (Vanhoutte *et al.*, 2005). In conclusion, we have demonstrated that rosuvastatin prevents endothelial dysfunction, vascular remodelling and changes in the ECM in small resistance arteries in Ang II-infused rats. These effects are likely to depend on a restoration of NO availability, reduction of intravascular ROS production by inhibition of Nox4/NAD(P)H oxidase and stimulation of endogenous antioxidant defences, and reversal of COX-1 induction/activity.

Because the activation of NAD(P)H oxidase and COX-1 pathways are recognized contributors to the Ang II-mediated atherosclerotic damage, their involvement may represent an explanation for the increased cardiovascular risk in patients treated with selective COX-2 inhibitors, as emerged in the past (Pratico and Dogne, 2005). Accordingly, the down-regulation of such determinants represents crucial mechanisms whereby statins may prevent the progression of cardiovascular disease, particularly in those forms of human hypertension characterized by elevated activity of the renin-angiotensin-aldosterone system, even in the presence of a normal lipid pattern.

Sources of funding

This work was partly supported by an institutional research grant issued by the Interdepartmental Centre for Research in Clinical Pharmacology and Experimental Therapeutics, University of Pisa, Italy.

Conflict of interest

None.

References

Ago T, Kitazono T, Ooboshi H, Iyama T, Han YH, Takada J *et al.* (2004). Nox4 as the major catalytic component of an endothelial NAD(P)H oxidase. Circulation 109: 227–233.

Alexander SPH, Mathie, A. Peters JA (2011). Guide to Receptors and Channels (GRAC), 5th edn. Br J Pharmacol 164 (Suppl. 1): S1-S324.

Bernini G, Galetta F, Franzoni F, Bardini M, Taurino C, Moretti A *et al.* (2008). Normalization of catecholamine production following resection of phaeochromocytoma positively influences carotid vascular remodelling. Eur J Endocrinol 159: 137–143.

Beswick RA, Dorrance AM, Leite R, Webb RC (2001). NADH/NADPH oxidase and enhanced superoxide production in the mineralocorticoid hypertensive rat. Hypertension 38: 1107–1111.

Bostom AG, Rosenberg IH, Silbershatz H, Jacques PF, Selhub J, D'Agostino RB *et al.* (1999). Nonfasting plasma total homocysteine levels and stroke incidence in elderly persons: the Framingham Study. Ann Intern Med 131: 352–355.

Brassard P, Amiri F, Schiffrin EL (2005). Combined angiotensin II type 1 and type 2 receptor blockade on vascular remodeling and matrix metalloproteinases in resistance arteries. Hypertension 46: 598–606.

Briones AM, Rodriguez-Criado N, Hernanz R, Garcia-Redondo AB, Rodrigues-Diez RR, Alonso MJ *et al.* (2009). Atorvastatin prevents angiotensin II-induced vascular remodeling and oxidative stress. Hypertension 54: 142–149.

Calkin AC, Giunti S, Sheehy KJ, Chew C, Boolell V, Rajaram YS *et al.* (2008). The HMG-CoA reductase inhibitor rosuvastatin and the angiotensin receptor antagonist candesartan attenuate atherosclerosis in an apolipoprotein E-deficient mouse model of diabetes via effects on advanced glycation, oxidative stress and inflammation. Diabetologia 51: 1731–1740.

Cui W, Matsuno K, Iwata K, Ibi M, Katsuyama M, Kakehi T *et al.* (2009). NADPH oxidase isoforms and anti-hypertensive effects of atorvastatin demonstrated in two animal models. J Pharmacol Sci 111: 260–268.

Faraci FM, Didion SP (2004). Vascular protection: superoxide dismutase isoforms in the vessel wall. Arterioscler Thromb Vasc Biol 24: 1367–1373.

Fukui T, Ishizaka N, Rajagopalan S, Laursen JB, Capers Q 4th, Taylor WR *et al.* (1997). p22phox mRNA expression and NADPH oxidase activity are increased in aortas from hypertensive rats. Circ Res 80: 45–51.

Griendling KK, Minieri CA, Ollerenshaw JD, Alexander RW (1994). Angiotensin II stimulates NADH and NADPH oxidase activity in cultured vascular smooth muscle cells. Circ Res 74: 1141–1148.

Hsich E, Segal BH, Pagano PJ, Rey FE, Paigen B, Deleonardis J *et al.* (2000). Vascular effects following homozygous disruption of p47(phox): an essential component of NADPH oxidase. Circulation 101: 1234–1236.

Intengan HD, Schiffrin EL (2000). Structure and mechanical properties of resistance arteries in hypertension: role of adhesion molecules and extracellular matrix determinants. Hypertension 36: 312–318.

Intengan HD, Thibault G, Li JS, Schiffrin EL (1999). Resistance artery mechanics, structure, and extracellular components in spontaneously hypertensive rats: effects of angiotensin receptor antagonism and converting enzyme inhibition. Circulation 100: 2267–2275.

Kang BY, Mehta JL (2009). Rosuvastatin attenuates Ang II – mediated cardiomyocyte hypertrophy via inhibition of LOX-1. J Cardiovasc Pharmacol Ther 14: 283–291.

Li JM, Shah AM (2003). Mechanism of endothelial cell NADPH oxidase activation by angiotensin II. Role of the p47phox subunit. J Biol Chem 278: 12094–12100.

Li JM, Gall NP, Grieve DJ, Chen M, Shah AM (2002). Activation of NADPH oxidase during progression of cardiac hypertrophy to failure. Hypertension 40: 477–484.

McGrath J, Drummond G, McLachlan E, Kilkenny C, Wainwright C (2010). Guidelines for reporting experiments involving animals: the ARRIVE guidelines. Br J Pharmacol 160: 1573–1576.

Neves MF, Virdis A, Schiffrin EL (2003). Resistance artery mechanics and composition in angiotensin II-infused rats: effects of aldosterone antagonism. J Hypertens 21: 189–198.

Neves MF, Endemann D, Amiri F, Virdis A, Pu Q, Rozen R *et al.* (2004). Small artery mechanics in hyperhomocysteinemic mice: effects of angiotensin II. J Hypertens 22: 959–966.

Paravicini TM, Touyz RM (2008). NADPH oxidases, reactive oxygen species, and hypertension: clinical implications and therapeutic possibilities. Diabetes Care 31 (Suppl 2): S170–S180.

Park JK, Mervaala EM, Muller DN, Menne J, Fiebeler A, Luft FC *et al.* (2009). Rosuvastatin protects against angiotensin II-induced renal injury in a dose-dependent fashion. J Hypertens 27: 599–605.

Pratico D, Dogne JM (2005). Selective cyclooxygenase-2 inhibitors development in cardiovascular medicine. Circulation 112: 1073–1079.

Rey FE, Cifuentes ME, Kiarash A, Quinn MT, Pagano PJ (2001). Novel competitive inhibitor of NAD(P)H oxidase assembly attenuates vascular O(2)(-) and systolic blood pressure in mice. Circ Res 89: 408–414.

Sicard P, Acar N, Gregoire S, Lauzier B, Bron AM, Creuzot-Garcher C *et al.* (2007). Influence of rosuvastatin on the NAD(P)H oxidase activity in the retina and electroretinographic response of spontaneously hypertensive rats. Br J Pharmacol 151: 979–986.

de Sotomayor MA, Perez-Guerrero C, Herrrera MD, Jimenez L, Marin R, Marhuenda E *et al.* (2005). Improvement of age-related endothelial dysfunction by simvastatin: effect on NO and COX pathways. Br J Pharmacol 146: 1130–1138.

Touyz RM, Schiffrin EL (2000). Signal transduction mechanisms mediating the physiological and pathophysiological actions of angiotensin II in vascular smooth muscle cells. Pharmacol Rev 52: 639–672.

Touyz RM (2005). Molecular and cellular mechanisms in vascular injury in hypertension: role of angiotensin II. Curr Opin Nephrol Hypertens 14: 125–131.

Touyz RM, Tabet F, Schiffrin EL (2003). Redox-dependent signalling by angiotensin II and vascular remodelling in hypertension. Clin Exp Pharmacol Physiol 30: 860–866.

Vanhoutte PM, Feletou M, Taddei S (2005). Endothelium-dependent contractions in hypertension. Br J Pharmacol 144: 449–458.

Virdis A, Neves MF, Amiri F, Viel E, Touyz RM, Schiffrin EL (2002). Spironolactone improves angiotensin-induced vascular changes and oxidative stress. Hypertension 40: 504–510.

Virdis A, Iglarz M, Neves MF, Amiri F, Touyz RM, Rozen R *et al.* (2003). Effect of hyperhomocysteinemia and hypertension on endothelial function in methylenetetrahydrofolate reductase-deficient mice. Arterioscler Thromb Vasc Biol 23: 1352–1357.

Virdis A, Neves MF, Amiri F, Touyz RM, Schiffrin EL (2004). Role of NAD(P)H oxidase on vascular alterations in angiotensin II-infused mice. J Hypertens 22: 535–542.

Virdis A, Colucci R, Fornai M, Blandizzi C, Duranti E, Pinto S *et al.* (2005). Cyclooxygenase-2 inhibition improves vascular endothelial dysfunction in a rat model of endotoxic shock: role of inducible nitric-oxide synthase and oxidative stress. J Pharmacol Exp Ther 312: 945–953.

Virdis A, Colucci R, Fornai M, Duranti E, Giannarelli C, Bernardini N *et al.* (2007). Cyclooxygenase-1 is involved in endothelial dysfunction of mesenteric small arteries from angiotensin II-infused mice. Hypertension 49: 679–686.

Virdis A, Colucci R, Versari D, Ghisu N, Fornai M, Antonioli L *et al.* (2009). Atorvastatin prevents endothelial dysfunction in mesenteric arteries from spontaneously hypertensive rats: role of cyclooxygenase 2-derived contracting prostanoids. Hypertension 53: 1008–1016.

Virdis A, Colucci R, Neves MF, Rugani I, Aydinoglu F, Fornai M *et al.* (2012). Resistance artery mechanics and composition in angiotensin II-infused mice: effects of cyclooxygenase-1 inhibition. Eur Heart J 33: 2225–2234.

Whaley-Connell A, Habibi J, Nistala R, Cooper SA, Karuparthi PR, Hayden MR *et al.* (2008). Attenuation of NADPH oxidase activation and glomerular filtration barrier remodeling with statin treatment. Hypertension 51: 474–480.

Supporting information

Additional Supporting Information may be found in the online version of this article at the publisher's web-site:

Figure S1 Systolic, diastolic and mean blood pressure time courses in control, Ang II-infused and Ang II-infused-rosuvastatin-treated rats (n = 6 animals for each group). Results are given as mean ± SEM. *P<0.001 versus other groups (whole curve); †P<0.05 versus Ang II (whole curve).

Figure S2 Relaxations to acetylcholine (A) or sodium nitroprusside (B) in mesenteric resistance arteries from Ang II-treated rats at baseline (saline) or under acute incubation with incremental concentrations of rosuvastatin. Results are given as the mean of 6 animals ± SEM. *P<0.05; †P<0.01.

Figure S3 (A) Representative images of full gels from immunoprecipitation (IP) with anti-p47phox antibody followed by immunoblotting (IB) for phosphoserine, p67phox and p47phox in small vessels from control and Ang II-infused rats ± rosuvastatin (Rosu). (B) Representative image of immunoblotting for β-actin in total lysates from control and Ang II-infused rats with or without rosuvastatin (Rosu).

Table S1 Functional and morphological vascular parameters from Ang II-infused rats treated with incremental doses of simvastatin, atorvastatin or rosuvastatin for 2 weeks.

Appendix S1 Preparation, mounting, measurements and mechanics in small mesenteric arteries.